Mathematical Modeling of Free-Radical Polymerization Fronts

P. M. Goldfeder and V. A. Volpert*

Department of Engineering Sciences and Applied Mathematics, Northwestern University, Evanston, Illinois 60208

V. M. Ilyashenko,† A. M. Khan, J. A. Pojman, and S. E. Solovyov

Department of Chemistry and Biochemistry, University of Southern Mississippi, Hattiesburg, Mississippi 39406-5043

Received: July 17, 1996; In Final Form: January 22, 1997[⊗]

Frontal polymerization is a process in which a spatially localized reaction zone propagates into a monomer, converting it into a polymer. In the simplest case of free-radical polymerization, a mixture of a monomer and initiator is placed into a test tube. Upon reaction initiation at one end of the tube, a self-sustained thermal wave, in which chemical conversion occurs, develops and propagates through the tube. We develop a mathematical model of the frontal polymerization process and analytically determine the structure of the polymerization wave, the propagation velocity, maximum temperature, and degree of conversion of the monomer. Specifically, we examine their dependence on the kinetic parameters of the reaction, the initial temperature of the mixture, and the initial concentrations of the initiator and monomer. Our analytic results are in good quantitative agreement with both direct numerical simulations of the model and experimental data (on butyl acrylate polymerization), which are also presented in the paper.

I. Introduction

Frontal polymerization is a process in which a spatially localized reaction zone propagates into a monomer, converting it into a polymer. This paper will concentrate on *exothermic* frontal polymerization processes such as methacrylic acid and butyl acrylate polymerization. In the simplest case of free-radical polymerization, a mixture of a monomer and initiator is placed into a test tube. Upon reaction initiation at one end of the tube a self-sustained thermal wave, in which chemical conversion occurs, develops and propagates through the tube.

Studies of frontal polymerization began in 1972 in the former Soviet Union.[1−4] They studied frontal polymerization of methyl methacrylate and discussed how various factors such as the initial temperature and concentrations, ambient pressure, the nature of the initiator, etc., affected the characteristics of the propagating wave, its velocity, and the composition of the polymer. Polymerization waves were also observed for the curing of epoxy resins.[5] The main goal of these works was to demonstrate in principle the possibility for a polymerization process to occur in the frontal mode. Later work by several other groups confirmed these findings (see, e.g., the references in refs 6 and 7), and there is currently extensive experimental work being done on frontal polymerization.[8−14]

The importance of studies of frontal polymerization is twofold. First, it is a method to produce polymers that bears a strong resemblance to another technological process occurring in a frontal regime, namely, self-propagating high-temperature synthesis (SHS). The SHS process uses combustion waves to synthesize desired inorganic materials[15−17] in a way very similar to the polymerization front discussed above. In the simplest manifestation of this process, a sample made of a powder mixture is ignited at one end and the reaction propagates through the reactants by a high-temperature thermal wave of frontal structure, which leaves products in its wake. The SHS process has a number of benefits over the commonly used batch method of product formation. One significant advantage is the savings in energy cost. SHS utilizes, rather than wastes, the internal energy of the reactants themselves. Other process improvements include a shorter reaction time, the use of more simple production equipment, and an improved product purity as the high temperature achieved by SHS burns off many impurities. We expect that similar benefits can be achieved if this approach is applied to polymer synthesis. Energy costs and waste solvent production could be minimized while product purity is maximized. Before any of these advantages can be achieved, a better understanding of the factors that affect frontal polymerization is necessary.

Second, frontal polymerization studies can lead to a greater understanding of the fundamental mechanisms involved in reaction wave propagation in general. A polymerization wave, though having some unique features, is definitely a reaction wave.[18−27]

In this paper we develop and study a mathematical model of the propagation of free-radical polymerization fronts. We do this by examining the kinetic equations and energy balance in order to analytically determine the structure of the polymerization wave, its propagation velocity, maximum temperature, and degree of conversion of the monomer. We analyze how these quantities are affected by the kinetic parameters of the reactions as well as by the initial temperature of the mixture and concentrations of the initiator and the monomer. In addition to these theoretical findings, experimental and numerical results will be presented and compared.

II. Mathematical Model

The propagation of free-radical polymerization fronts involves the usual free-radical mechanism with a number of chemical steps,[28] a simplified description of which follows. First, the initiator, which is thermally unstable, decomposes due to the heat produced in the system yielding two radicals (R)

$$I \xrightarrow{k_d} f \times 2R$$

† Present address: Boston Optical Fibers, Westborough, MA 01581.

[⊗] Abstract published in *Advance ACS Abstracts,* April 1, 1997.

S1089-5647(96)02150-5 CCC: $14.00

(decomposition step) where f is the efficiency factor which depends on the type of initiator. We use $f = 0.5$ as a typical value of the efficiency factor. A radical can then combine with a monomer to initiate a polymer chain P_1 (initiation step)

$$R + M \xrightarrow{k_p} P_1$$

which then grows (propagation step)

$$P_n + M \xrightarrow{k_p} P_{n+1}$$

Here P_n, $n = 1, 2, ...$, is a polymer radical which includes n monomer molecules. The propagation step continues until it terminates by either the reaction between two polymer radicals

$$P_n + P_m \xrightarrow{k_t} P$$

or the reaction between the polymer radical and the initiator radical

$$P_n + R \xrightarrow{k_t} P$$

(termination step). Here P is a molecule of the polymer which is no longer chemically active. Reaction constants are taken in the form of Arrhenius exponentials

$$k_d = k_d^0 \exp(-E_d/R_gT), \quad k_p = k_p^0 \exp(-E_p/R_gT), \quad k_t = k_t^0 \exp(-E_t/R_gT)$$

where R_g is the gas constant, T is the temperature of the mixture, and k_d^0, k_p^0, k_t^0 and E_d, E_p, E_t are the frequency factors and activation energies of the decomposition, propagation, and termination steps, respectively.

The characteristic scale of the polymerization wave is typically much smaller than the length of the tube, so that a traveling wave coordinate (x) may be introduced, and the kinetic equations are written as

$$uI' + k_dI = 0 \tag{2.1}$$

$$uR' - 2fk_dI + k_pRM + k_tR\dot{P} = 0 \tag{2.2}$$

$$uM' + k_pRM + k_pM\dot{P} = 0 \tag{2.3}$$

$$u\dot{P}' - k_pRM + k_tR\dot{P} + k_t\dot{P}^2 = 0 \tag{2.4}$$

$$uP' - k_tR\dot{P} - k_t\dot{P}^2 = 0 \tag{2.5}$$

where u is the propagation velocity of the wave which must be determined in the course of solution of the problem. Here I, R, M, and P denote the concentrations in mol/L of the corresponding species, $\dot{P}$ is the concentration of the polymer radicals, and the prime denotes the derivative with respect to x. These kinetic equations must be supplemented by the energy balance in the system, which accounts for thermal diffusion and heat release in the polymerization process. Since the heat release occurs mainly in the propagation step,[29] the energy balance takes the form

$$\kappa T'' - uT' + qk_p(RM + M\dot{P}) = 0 \tag{2.6}$$

where κ is the thermal diffusivity of the mixture (assumed to be constant), and $q = -\Delta H/(c\rho)$, where ΔH is the reaction enthalpy, and ρ and c are the mixture density and specific heat, respectively, also assumed to be constant.

The boundary conditions for the system (2.1)−(2.6) are the initial state far ahead of the polymerization wave ($x \to -\infty$), and the final state behind the wave ($x \to \infty$), where all of the reactions have come to completion

$$x \to -\infty: T = T_0, \quad I = I_0, \quad R = 0, \quad M = M_0, \quad P = 0, \quad \dot{P} = 0$$

$$x \to \infty: \ T' = 0 \tag{2.7}$$

We will study a simplified kinetic system by using a steady state assumption regarding the total concentration of the radicals, including both the initial (R) and polymer ($\dot{P}$) radicals. This means that the rate of change of the concentration of the radicals is much smaller than the rates of their production and consumption, so that there is a simple algebraic balance between the amounts of radicals and initiator. This assumption reduces equations 2.2−2.4 to the single equation

$$uM' + k_{eff}\sqrt{IM} = 0 \tag{2.8}$$

and the energy balance (2.6) to

$$\kappa T'' - uT' + qk_{eff}\sqrt{IM} = 0 \tag{2.9}$$

where the effective reaction constant k_{eff} is given by

$$k_{eff} = k_{eff}^0 \exp(-E_{eff}/R_gT), \quad k_{eff}^0 = k_p^0[2fk_d^0/k_t^0]^{1/2}, \quad E_{eff} = E_p + (E_d - E_t)/2$$

The steady state assumption has been justified in the case of constant, low-temperature polymerization,[30] as well as for nonisothermal bulk polymerization.[31,32]

Thus, our mathematical model consists of the mass and heat balances (2.1), (2.8), and (2.9) and boundary conditions describing the initial state far ahead of the polymerization wave and the final state far behind the wave. For calculational simplicity, we make a change of variables for the initiator, $I = J^2$, and for convenience rewrite the equations as

$$uJ' + Jk_1(T) = 0 \tag{2.10}$$

$$uM' + JM\chi(J_0 - J)k_2(T) = 0 \tag{2.11}$$

$$\kappa T'' - uT' + qJM\chi(J_0 - J)k_2(T) = 0 \tag{2.12}$$

and the boundary conditions at the cold ($x = -\infty$) and hot ($x = +\infty$) boundaries

$$x = -\infty: \ M = M_0, \quad T = T_0, \quad J = J_0 \tag{2.13}$$

$$x = +\infty: \ T' = 0 \tag{2.14}$$

Here T_0 is the initial temperature, J_0 and M_0 are the amount of initiator and monomer present in the initial mixture, and

$$k_1(T) = k_d(T)/2 = k_{01}e^{-E_1/R_gT}, \quad k_{01} = k_d^0/2, \quad E_1 = E_d$$

$$k_2(T) = k_{eff}(T) = k_{02}e^{-E_2/R_gT}, \quad k_{02} = k_{eff}^0, \quad E_2 = E_{eff}$$

Finally, $\chi(J_0-J)$ is the Heaviside function, i.e., it is equal to zero if $J \geq J_0$, and to 1 if $J < J_0$. This factor has been introduced in the polymerization reaction rate to make up for an inaccuracy of the steady state approximation that allows for the polymerization reaction to occur prior to the initiator decomposition, which is inconsistent with the nature of the polymerization model.

From eq 2.10 we can see that as $x \rightarrow \infty$, $J(x) \rightarrow 0$. Similarly, from eq 2.11 we can see that as $x \rightarrow \infty$, $M(x)$ will reach a constant, albeit nonzero value, which we will call M_b. By combining eqs 2.11 and 2.12 to eliminate the reaction term and integrating the result from $-\infty$ to ∞, we find that as $x \rightarrow \infty$ the temperature T reaches a constant value, which we will call T_b, where

$$T_b = T_0 + q(M_0 - M_b) \tag{2.15}$$

The quantities T_b and M_b are important characteristics of the polymerization process and they have to be determined.

Though frontal polymerization is much slower and significantly less exothermic than combustion processes, nondimensional parameters, such as $R_g T_b/E_1$ and $R_g T_b/E_2$, that determine the structure of the wave are of the same order as the corresponding small parameters in combustion problems. Thus, the methods developed in combustion theory can be used to attack the frontal polymerization problem. One such approach allows us to analytically study the problem by replacing the usual Arrhenius dependence of the reaction rate on temperature, $k_n(T)$ ($n = 1, 2$), with the step function

$$\hat{k}_n(T) = \begin{cases} 0, & T < T_n^* \\ A_n, & T > T_n^* \end{cases} \tag{2.16}$$

where

$$T_n^* = T_b(1 - \epsilon_n), \quad A_n = k_n(T_b), \quad \epsilon_n = R_g T_b/E_n \tag{2.17}$$

Here, T_n^* are the temperatures at which the first and second reactions begin, ϵ_n is a small dimensionless parameter, A_n is the height of the step function, and $k_n(T_b)$ is the reaction rate evaluated at the maximum temperature, T_b. Thus the actual Arrhenius temperature dependence is replaced by the step function with height equal to the maximum of the Arrhenius function. The integral values of the two over the range from T_0 to T_b are approximately equal. This approach has been successfully applied in a number of combustion problems (see, for example, ref 33). This use of a step function will be further discussed in the Appendix where, for the simpler case of a single chemical reaction, we compare the results of direct numerical simulations with Arrhenius temperature dependence to those with a step function approximation.

We are considering the case where the activation energy for the decomposition reaction, E_1, is greater than that for the polymerization reaction, E_2, though both reactions begin simultaneously due to the aforementioned Heaviside function, χ, in the polymerization reaction rate. Since the set of equations is invariant under spatial translation, we let the point in space where both reactions begin be $x = 0$. Because we have replaced the Arrhenius-type reaction rates with step functions, the spatial region from $x = -\infty$ to $x = +\infty$ can be divided into two regions: one where neither reaction has begun ($x < 0$, $k_1(T) = k_2(T) = 0$), and one in which both reactions have occurred ($x > 0$, $k_1(T)k_2(T) \neq 0$). Thus eqs 2.10−2.12 can be stated for each of the two regions as

$$uJ' = 0, \quad uM' = 0, \quad \kappa T'' - uT' = 0 \tag{2.18}$$

for $x < 0$, and

$$uJ' + J(x)A_1 = 0 \tag{2.19}$$

$$uM' + J(x)M(x)A_2 = 0 \tag{2.20}$$

$$\kappa T'' - uT' + qJ(x)M(x)A_2 = 0 \tag{2.21}$$

for $x > 0$. The boundary conditions are given in (2.13) and (2.14). In addition, there are the following matching conditions at $x = 0$ that constitute continuity of the mass, temperature, and temperature gradient distributions in the polymerization wave:

$$J|_{x=0^-} = J|_{x=0^+} \tag{2.22}$$

$$M|_{x=0^-} = M|_{x=0^+} \tag{2.23}$$

$$T|_{x=0^-} = T|_{x=0^+} = T_1^* \tag{2.24}$$

$$T'|_{x=0^-} = T'|_{x=0^+} \tag{2.25}$$

The last condition in (2.24) states that the reactions start at $x = 0$, i.e., the temperature reaches the value T_1^* at this point.

III. Solution

Solution of the eqs 2.18 in the $x < 0$ region, satisfying the boundary conditions (2.13), as well as the second condition in (2.24) can be readily found as

$$J(x) = J_0 \tag{3.1}$$

$$M(x) = M_0 \tag{3.2}$$

$$T(x) = T_0 + (T_1^* - T_0)e^{(u/\kappa)x} \tag{3.3}$$

Solution of eqs 2.19−2.21 in the $x > 0$ region satisfying the matching conditions (2.22)−(2.25) are given by

$$J(x) = J_0 e^{-(A_1/u)x} \tag{3.4}$$

$$M(x) = M_0 \exp\left[\frac{A_2 J_0}{A_1}(e^{-(A_1/u)x} - 1)\right] \tag{3.5}$$

$$T(x) = T_0 + qM_0\left(1 - \exp\left[\frac{A_2 J_0}{A_1}(e^{-(A_1/u)x} - 1)\right]\right) + \frac{A_2 q J_0 M_0}{u} \exp\left[\frac{u}{\kappa}x - \frac{A_2 J_0}{A_1}\right] I(x) \tag{3.6}$$

where

$$I(x) = \int_x^\infty \exp\left[\frac{A_2 J_0}{A_1} e^{-(A_1/u)t} - (A_1/u)t - (u/\kappa)t\right] dt \tag{3.7}$$

These equations involve an unknown propagation velocity u and, implicitly, both the burning temperature T_b and the amount of unreacted monomer M_b. Taking the limit as $x \rightarrow \infty$ in (3.5) and (3.6), we find

$$M_b = M_0 e^{-(A_2 J_0/A_1)} \tag{3.8}$$

$$T_b = T_0 + q(M_0 - M_b) \tag{3.9}$$

Using the second equation in (2.24) we find

$$T_b(1 - \epsilon_1) = T_0 + qM_0 \frac{A_2 J_0}{u} I(0) e^{-(A_2 J_0/A_1)} \tag{3.10}$$

Thus, we have derived three equations, (3.8), (3.9), and (3.10), for the three unknown quantities u, T_b, and M_b. Notice that eq 3.9 is identical to eq 2.15 above, as would be expected. To

study these equations it is convenient to define the following nondimensional variables

$$\upsilon = \kappa A_2 J_0/u^2, \quad m = M_b/M_0, \quad \alpha = A_2 J_0/A_1 \quad (3.11)$$

where υ is related to the propagation velocity, m is the ratio of remaining monomer to initial monomer, and α measures the relative strength of the reaction rates. We can now rewrite eqs 3.8−3.10 as

$$m = 1 - \frac{T_b - T_0}{qM_0} \quad (3.12)$$

$$m = e^{-\alpha} \quad (3.13)$$

$$T_b(1 - \epsilon_1) = T_0 + qM_0 \upsilon e^{-\alpha} I \quad (3.14)$$

where the following variable was introduced:

$$I = \frac{u}{\kappa} I(0) = \frac{u}{\kappa} \int_0^\infty \exp\left[\alpha e^{-(A_1/u)t} - \frac{A_1}{u} t\right] e^{-(u/\kappa)t}\, dt = \frac{\alpha}{\upsilon} \int_0^1 e^{\alpha y} y^{\alpha/\upsilon}\, dy \quad (3.15)$$

We remark that as it follows from (3.13), m is necessarily greater than zero, so that the monomer is never completely consumed in the reaction. Eliminating m from (3.12) and (3.13) we derive an equation for T_b

$$e^{-\alpha} = 1 - \frac{T_b - T_0}{qM_0}$$

which can also be written in terms of the original parameters of the problem as

$$\left(\frac{2I_0^{1/2} k_p^0}{[k_d^0 k_t^0]^{1/2}}\right) \exp\left[\frac{E_t + E_d - 2E_p}{2R_g T_b}\right] = \ln\left(\frac{qM_0}{T_0 + qM_0 - T_b}\right) \quad (3.16)$$

We observe that the right-hand side of the equation increases from zero to infinity as T_b varies from T_0 to $T_0 + qM_0$ while the left-hand side is a decreasing function of T_b provided that $E_t + E_d > 2E_p$, which is the case for the typical parameter values given below in (5.1). In addition, replacing T_b by $T_0 + qM_0$ in the left-hand side of (3.16) and solving the resulting equation provides a lower bound for the actual value of T_b. This allows us to conclude that if the parameter values in (5.1) are used and I_0 is not too small, then T_b is very close to the adiabatic temperature $T_0 + qM_0$, and almost all of the monomer will be consumed. If either the kinetic parameters are different or I_0 is much smaller than the values currently used in experiments, then T_b will not necessarily be close to the adiabatic temperature. In this case (3.16) must be solved for T_b, and the amount of unreacted monomer, M_b, can then be found from either (3.12) or (3.13).

For the cases where the activation energies are such that $E_t + E_d < 2E_p$ then eq 3.16 may exhibit both multiple solutions and the critical phenomenon of their disappearance. It would be interesting to see if this case is just a mathematical curiosity or such polymerizing systems actually exist.

Next, when T_b is found, eq 3.14 can be used to determine the propagation velocity in the following way. Substituting (3.15) into eq 3.14,

$$T_b(1 - \epsilon_1) = T_0 + qM_0 e^{-\alpha} \alpha \int_0^1 e^{\alpha y} y^{\alpha/\upsilon}\, dy \quad (3.17)$$

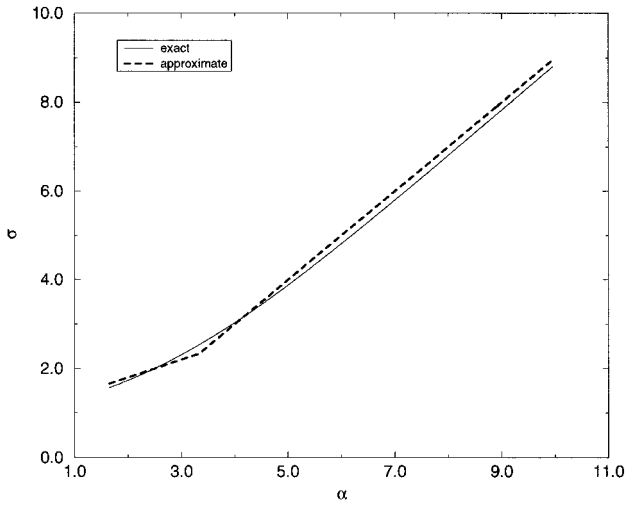

Figure 1. Plot of both the exact and approximate values of the parameter σ (see eqs 3.23 and 3.24) as functions of α.

Simplification via eqs 3.12 and 3.13 gives us

$$\epsilon_1 \frac{T_b}{qM_b} = e^{\alpha} - 1 - \alpha \int_0^1 e^{\alpha y} y^{\alpha/\upsilon}\, dy \quad (3.18)$$

Replacing $e^{\alpha} - 1$ with $\alpha \int_0^1 e^{\alpha y}\, dy$ and simplifying

$$\epsilon_1 \frac{T_b}{qM_b} = \alpha \int_0^1 e^{\alpha y}(1 - y^{\alpha/\upsilon})\, dy \quad (3.19)$$

Though this equation cannot be solved explicitly, by realizing that certain quantities are large and others are small, it can be solved approximately. The small parameter is ϵ, and the large one is υ. Realizing this, we can make the following assertion:

$$y^{\alpha/\upsilon} \sim 1 + (\alpha/\upsilon) \ln y \quad (3.20)$$

and rewrite eq 3.19 as

$$\epsilon_1 \frac{T_b}{qM_b} = \frac{\alpha^2}{\upsilon} \int_0^1 e^{\alpha y} \ln\left(\frac{1}{y}\right) dy \quad (3.21)$$

By substituting in results from eq 3.12, 3.13, and 3.21, as well as replacing υ with results from eq 3.11 we can find an expression for u, the propagation velocity

$$u^2 = \frac{\kappa A_1 R_g T_b^2}{E_1(T_b - T_0)} \sigma(\alpha) \quad (3.22)$$

where

$$\sigma(\alpha) = \frac{e^{\alpha} - 1}{\alpha \int_0^1 e^{\alpha y} \ln(1/y)\, dy} \quad (3.23)$$

We observe that $\sigma(\alpha) \sim \alpha$ for α large, $\sigma(\alpha) \sim 1$ for α small, and it can be accurately approximated as

$$\sigma(\alpha) \approx \begin{cases} \alpha - 1, & \alpha > 10/3 \\ 1 + 0.4\alpha, & \alpha < 10/3 \end{cases} \quad (3.24)$$

in the entire range of variation of α (see Figure 1). If α is large (corresponding to the case when the maximum temperature T_b is close to the adiabatic temperature $T_0 + qM_0$, initial concentrations of the initiator J_0 are not too small, and

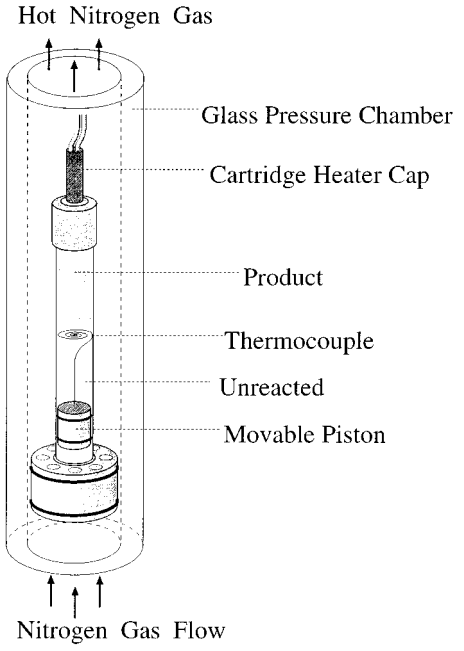

Figure 2. Experimental setup.

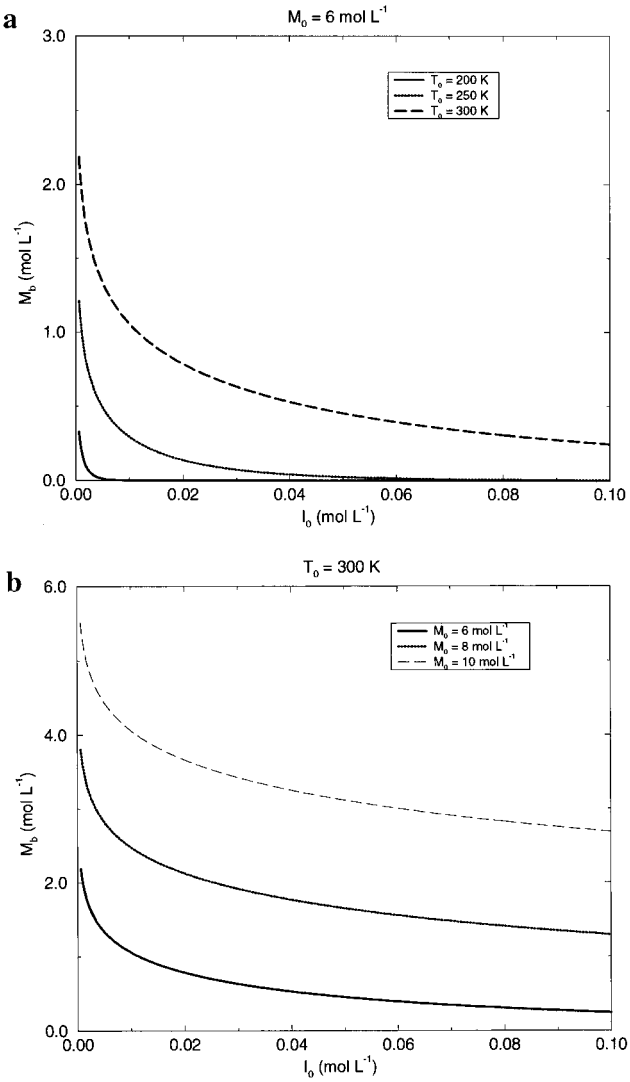

Figure 3. Effects of changes in (a) the initial temperature, and (b) the initial amount of monomer present on the amount of unreacted monomer remaining after the reactions have ceased.

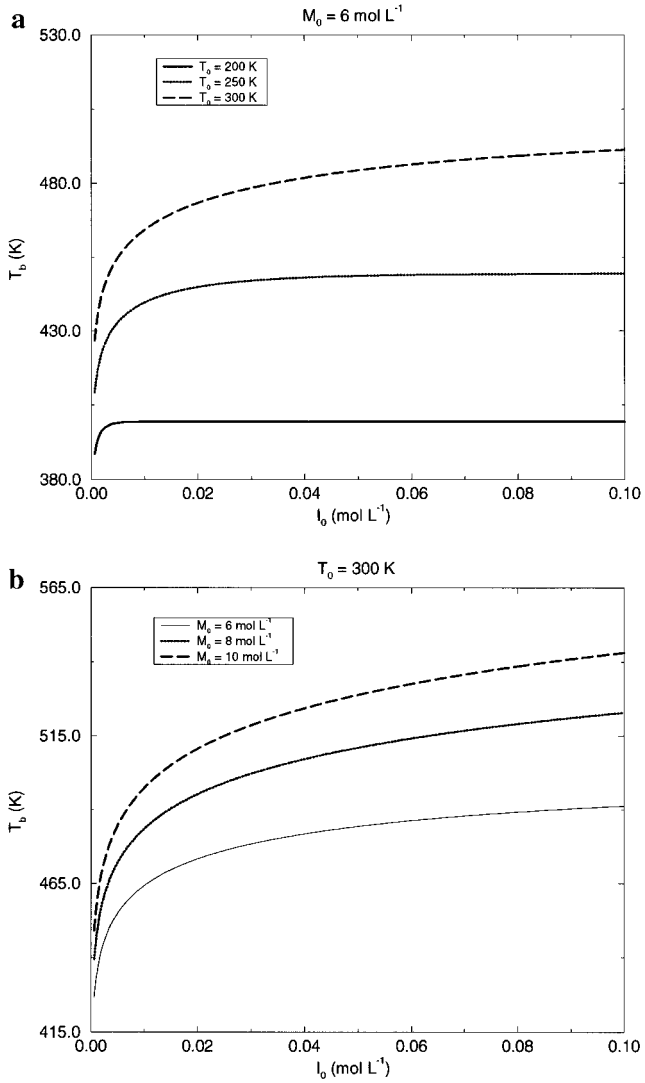

Figure 4. Effects of changes in (a) the initial temperature, and (b) the initial amount of monomer present on the maximum temperature of the system.

characteristic values of the kinetic parameters used) then the above asymptotics for σ reduce (3.22) to

$$u^2 = \frac{\kappa J_0 R_g T_b^2}{E_1(T_b - T_0)} k_{eff}^0 e^{-E_{eff}/R_g T_b} \qquad (3.25)$$

where T_b can be replaced by $T_0 + qM_0$. If α is sufficiently small, the use of the above asymptotics yields

$$u^2 = \frac{\kappa R_g T_b^2}{2E_1(T_b - T_0)} k_d^0 e^{-E_d/R_g T_b} \qquad (3.26)$$

where T_b is no longer close to $T_0 + qM_0$ and is determined by (3.16). The above approximation for σ allows one to also simplify (3.22) for intermediate values of α.

IV. Experimental Studies

The experimental results discussed in this paper were obtained using a setup consisting of a vertical glass tube filled with a monomer, butyl acrylate, and a thermal initiator, AIBN. The front was initiated at the end of the tube thermally, by heat from a cartridge heater.

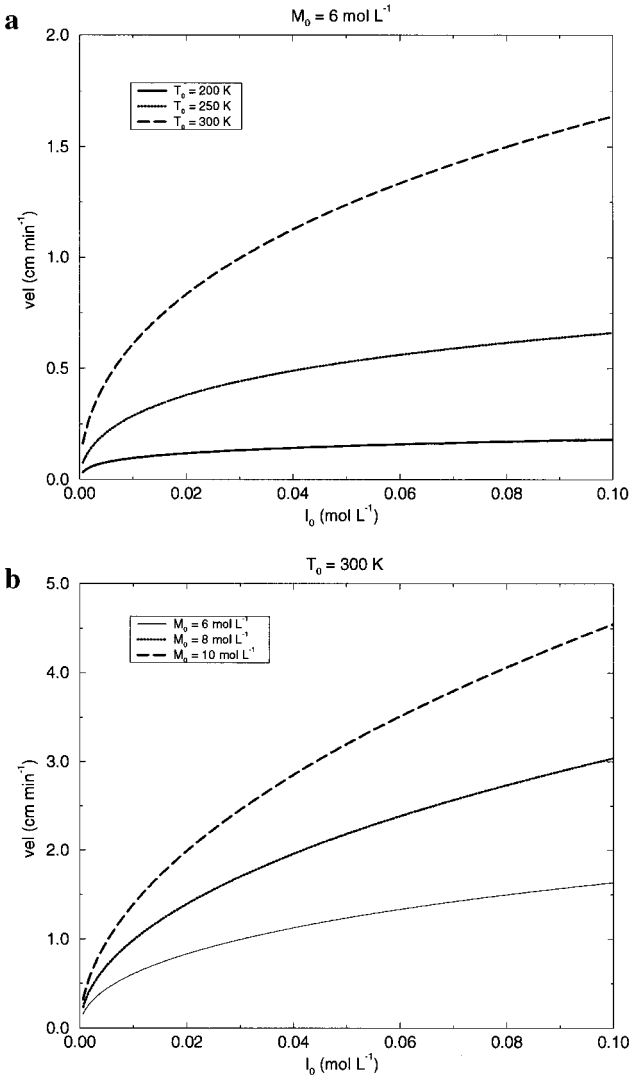

Figure 5. Effects of changes in (a) the initial temperature, and (b) the initial amount of monomer present on the propagation velocity.

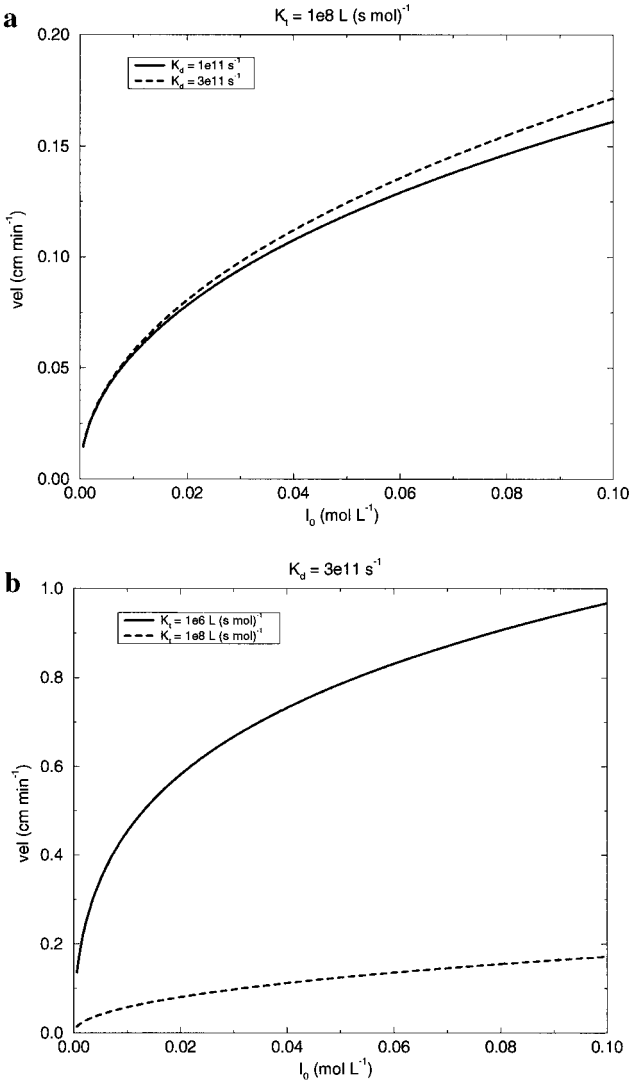

Figure 6. Effects of changes in (a) the decomposition reaction constant, and (b) the termination reaction constant on the propagation velocity.

Early experiments showed that the propagation velocity was typically increased by the presence of bubbles formed under the front as a result of initiator decomposition. These bubbles affect the velocity by forcing unreacted monomer up and around the cooling area, contracting the polymer plug.[9,11] The velocity of fronts in standard closed test tubes initially at ambient pressure were found to be as much as 30% higher than those fronts free of bubbles. To determine the true front velocity requires that the effect of bubbles be eliminated. Different initiators can yield different amounts of gas. Thus, the velocity depends not only on the kinetics of the initiator decomposition but also on the amount of gas produced and on the applied pressure. By performing the experiments in a pressure reactor, the formation of bubbles can be minimized, allowing for more accurate measurements of the velocity dependence on the initial temperature and initiator concentration. Experiments were performed in a custom-built reactor of our design that allowed isobaric (up to 50 atm pressure) conditions and controlled initial temperatures (Figure 2).

For pressure (up to 50 atm) experiments the reaction vessel was placed in an all-glass pressurized chamber and oriented in such a manner that the sealed end was at the top and the open end in the downward direction (Figure 2). A movable air-tight piston at the open end contained the reactants. An increase of pressure in the pressure chamber caused the piston to move inwards in the reaction tube and vice versa to compensate for any resulting pressure difference between the chamber and the reaction tube. A subminiature thermocouple probe (Omega TMQSS-0.020(G)-12") passed through the piston and was formed into a spiral parallel to the front surface for temperature profile measurements.

The pressurized chamber was submerged in a large temperature-controlled water bath equipped with an oblong window. Fronts were initiated by a cartridge heater in the metal cap on top of the tube. A motorized video camera monitored the downward propagating front in the reaction chamber. A mass flow controller (Omega FMG 7201) maintained a 100 cm^3 min^{-1} nitrogen flow upwards along the sides of the reaction vessel to prevent an increase in temperature in the pressure chamber. The nitrogen was equilibrated to the water bath temperature via a copper coil before entering the chamber.

We remark that double-diffusive and Taylor instabilities can interfere with front propagation, especially with butyl acrylate because the product is molten at the front temperature.[11] Thus, ultrafine silica gel (Cabosil) was added to increase the viscosity.

Butyl acrylate was of reagent grade (Aldrich) and used without further purification. AIBN from Pfaltz and Bauer was recrystallized from methanol before use.

Several factors affect the reproducibility of the fronts but the most important one is a slow occurrence of the homogeneous

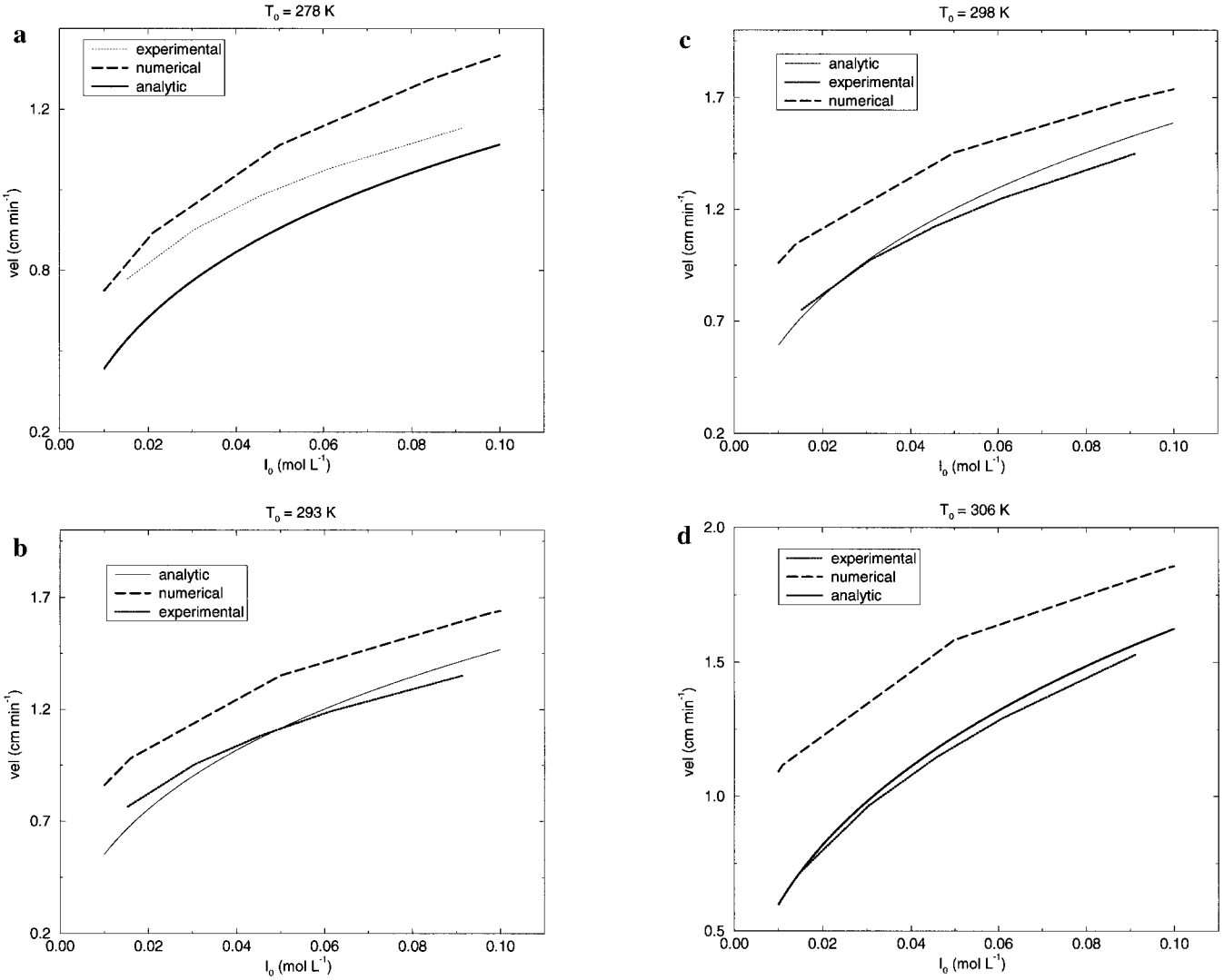

Figure 7. Comparison of the velocity curves attained analytically, experimentally, and numerically for initial temperatures of (a) 278 K, (b) 293 K, (c) 298 K, and (d) 308 K.

reaction ahead of the polymerization front, which consumes both the initiator and the monomer. We estimate the uncertainty in our measurements to be ±10%. Results of these experiments will be presented and discussed below.

V. Results

In this section we will discuss how variation of the initial temperature of the monomer, initiator concentration, kinetic parameters, etc., affect the maximum temperature in the front, the final degree of conversion of the monomer, the propagation velocity, and other quantities of interest. These results have been obtained in three ways: by examining eqs 3.16 and 3.22 (analytic approach), by direct numerical simulations of the mathematical model (numerical approach), and by performing experiments that used the experimental setup discussed above. The results given by the three approaches will be compared.

The numerical simulations were performed on the nonstationary version of the problem (2.10)−(2.14) without the Heaviside function introduced in these equations, using a finite difference scheme with adapting space grids for the integration. Implicit methods were used whenever possible and iterations were performed on each time step to ensure convergence of the solutions. The resulting systems of linear equations with tridiagonal matrices were solved using Thompson's algorithm.

Unless otherwise noted, the following parameter values were used in the analytic and numerical methods:

$$k_d^0 = 4 \times 10^{12}\ 1/\text{s}, \quad k_p^0 = 5 \times 10^6\ \text{L/(s·mol)}, \quad k_t^0 = 3 \times 10^7\ \text{L/(s·mol)}$$

$$E_d = 27\ \text{kcal/mol}, \quad E_p = 4.7\ \text{kcal/mol}, \quad E_t = 0.7\ \text{kcal/mol}$$

$$q = 33.24\ \text{L·K/mol}, \quad \kappa = 0.0014\ \text{cm}^2/\text{s} \qquad (5.1)$$

We have chosen parameters that are reasonable for addition polymerization[34] and have not used those recently reported for butyl acrylate[35] because they were derived from experiments performed at low temperatures.

Figures 3−6 show the effects that changes in the initial temperature (T_0), the amount of monomer initially present (M_0), and the kinetic parameters will have on the conversion of the monomer (M_b), the final temperature (T_b), and the propagation velocity. Figure 7a−d compares these analytic results with the numerical simulations and experimental data.

Figures 3 and 4 can best be understood by examining eq 3.9

$$T_b = T_0 + q(M_0 - M_b)$$

Since T_0, q, and M_0 are all constants, T_b will only change as

long as M_b is nonzero. Once the monomer has all been converted, the burning temperature will reach a constant value, regardless of change in the amount of initiator, I_0. In Figures 3a and 4a, the effect of changes in the initial temperature of the reaction, T_0, are evident. For lower temperatures, the monomer is completely consumed for even small amounts of initiator. But for temperatures at or above room temperature, complete conversion does not take place.

Figures 3b and 4b show the effect that changing M_0 will have on M_b and T_b. The results of Figure 3b are somewhat intuitive: the more monomer initially present, the more initiator required to polymerize it. An interesting observation about Figure 4b is that the distance between the top and middle curves is greater than that between the middle and bottom curves. It might be expected that because the increase in M_0 is the same from one curve to the next, then so should the distance between the curves. The reason that this is not true can best be seen by looking at eq 3.8

$$M_b = M_0 e^{-(A_2 J_0/A_1)}$$

The amount of monomer remaining, and thus the final temperature, are exponentially dependent on the amount of initiator. Thus, the relationship between the curves will change as a function of both M_0 and J_0.

Figure 5a,b illustrates how the front velocity is affected by changes in T_0 and M_0. Figure 5a shows the anticipated result that the higher the temperature of the system, the faster the front will propagate. Figure 5b can be understood by realizing that the more monomer reacting, the greater the velocity will be. Thus, increases in M_0, and thus M_b, will be accompanied by increase in the speed of the front.

Figure 6a,b shows how changes in some of the kinetic parameters involved in the reaction affect the front velocity. Changes in the reaction constant involving the decomposition of the initiator have little effect on the velocity. Changing k_d^0 will cause some change in the velocity, but it will be slight. Increasing this parameter will cause increases in the velocity. The reason for this is that as more initiator decomposes, more radicals will be produced. These radicals will then be able to combine with monomers to produce more polymers. The more polymerization taking place, the greater the velocity. Changes in the reaction constant involving the termination step of the reaction have a much more significant effect. If the reaction terminates, then polymerization will cease and the velocity will drop toward zero.

The results shown in Figure 7 help to justify the validity of the mathematical model derived above. The experimental, numerical, and analytic results are all in good agreement, especially for higher values of the initial temperature. This is expected, since parameter values in the analytic and numerical models were chosen to match the experimental findings.

We have introduced a mathematical model of the free-radical polymerization process. From this model, expressions were found for the propagation velocity, maximum temperature, and degree of monomer converted. Although simplifying assumptions were made, agreement with direct numerical simulations and experimental data was good.

Acknowledgment. This research has been supported in part by NSF Grants CTS 9308708, CTS 9319175, DMS 9600103 and by NSF's Mississippi EPSCoR Program.

Appendix

In order to justify the use of a step function in place of the usual Arrhenius-type temperature dependence, consider a simpler problem: a general first-order combustion reaction. Propagation of the combustion wave in this case is described by the system of two equations

$$\kappa T'' - uT' + qk(T)a = 0 \tag{A.1}$$

$$-ua' - k(T)a = 0 \tag{A.2}$$

where T is the temperature, u is the propagation velocity, q is the heat release in the reaction, a is the concentration of the reactant, and $k(T)$ is the temperature dependence of the reaction rate,

$$k(T) = k_0 e^{-E/R_g T}$$

Here, E is the activation energy and k_0 is the preexponential factor. The system of equations is considered on the entire x-axis subject to the boundary conditions

$$x \to -\infty:\ T = T_0,\ a = 1 \tag{A.3}$$

$$x \to \infty:\ T' = 0 \tag{A.4}$$

where T_0 is the initial temperature.

Similarly to the system discussed in the body of this paper, we replace the usual Arrhenius temperature dependence by a step function:

$$\hat{k}(T) = \begin{cases} 0, & T < T_b(1-\epsilon) \\ A, & T > T_b(1-\epsilon) \end{cases} \tag{A.5}$$

where

$$A = k(T_b),\quad T_b = T_0 + q,\quad \epsilon = R_g T_b/E \tag{A.6}$$

Here, T_b is the burnt fuel temperature and ϵ is a small dimensionless parameter. The step function temperature dependence divides the entire axis into two distinct regions: one where the reaction has not yet begun ($T < T_b(1-\epsilon)$) and one where the reaction occurs ($T > T_b(1-\epsilon)$). Because the system is invariant under spatial translation, we can name the point in space separating these two regions as $x = 0$, so that the system reduces to

$$\kappa T'' - uT' = 0,\quad -ua' = 0 \quad (x < 0) \tag{A.7}$$

$$\kappa T'' - uT' + qaA = 0,\quad -ua' - Aa = 0 \quad (x > 0) \tag{A.8}$$

with the matching conditions

$$T|_{x=0^-} = T|_{x=0^+},\quad T'|_{x=0^-} = T'|_{x=0^+},\quad a|_{x=0^-} = a|_{x=0^+} \tag{A.9}$$

Solving eqs A.7 and A.8 and applying matching and boundary conditions yields

$$T(x) = T_0 + \frac{\kappa qA}{\kappa A + u^2} e^{(u/\kappa)x},\quad a(x) = 1 \quad (x < 0) \tag{A.10}$$

$$T(x) = T_0 + q - \frac{qu^2}{\kappa A + u^2} e^{-(A/u)x},\quad a(x) = e^{-(A/u)x} \quad (x > 0) \tag{A.11}$$

$$T_b(1-\epsilon) = T_0 + \frac{\kappa qA}{\kappa A + u^2} \tag{A.12}$$

Solving this for u^2 and using (A.6) we obtain

$$u^2 = \frac{\kappa k(T_b)\gamma}{1-\gamma},\quad \gamma \equiv \frac{RT_b^2}{Eq} \tag{A.13}$$

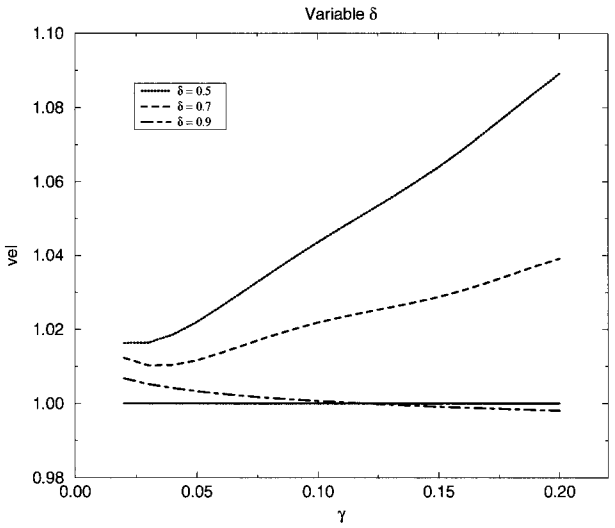

Figure 8. Effect of changes in the parameter γ (see eq A.13) on the nondimensional velocity, v (see eq A.19).

Since $\gamma \ll 1$, eq A.13 can be approximated as

$$u^2 = \kappa k(T_b)\frac{RT_b^{\,2}}{Eq} \tag{A.14}$$

In order to examine the validity of our use of a step function in place of the usual Arrhenius dependence, we solve eqs A.1 and A.2 numerically and compare the results to eq A.14. We do this by first combining eqs A.1 and A.2 to get

$$\kappa T'' - uT' - qua' = 0 \tag{A.15}$$

Integrating this equation and using the boundary conditions yields

$$\kappa T' - uT - qua = -uT_b \tag{A.16}$$

Combining this with eq A.2 gives us an equation for a as a function of T

$$\frac{u^2}{\kappa}\frac{da}{dT} = \frac{ak(T)}{T_b - T - qa}, \quad a(T_0) = 1, \quad a(T_b) = 0 \tag{A.17}$$

Introducing the following nondimensional variables and parameters

$$\theta = \frac{1}{\gamma}\frac{T - T_b}{q}, \quad \delta = \frac{q}{T_b}, \quad v^2 = \frac{u^2}{\kappa k(T_b)\gamma} \tag{A.18}$$

we can write eq A.17 as

$$v^2\frac{da}{d\theta} = -\frac{ae^{\theta/(1+\gamma\delta\theta)}}{a + \gamma\theta} \tag{A.19}$$

Figure 8 compares the approximate expression (A.14) for the propagation velocity with the numerical results obtained by solving (A.19). The straight line (vel = 1) is the approximate solution, while the three curves are the exact solution for three physically reasonable values of δ. Agreement between the approximate and exact solutions is very good, with a maximum error of less than 10%.

References and Notes

(1) Chechilo, N. M.; Khvilivitsky, R. Ya.; Enikolopyan, N. S. *Dokl. Phys. Chem.* **1972**, *204*, 512−513.
(2) Chechilo, N. M.; Enikolopyan, N. S. *Dokl. Phys. Chem.* **1974**, *214*, 174−176.
(3) Chechilo, N. M.; Enikolopyan, N. S. *Dokl. Phys. Chem.* **1975**, *221*, 391−394.
(4) Chechilo, N. M.; Enikolopyan, N. S. *Dokl. Phys. Chem.* **1976**, *230*, 840−843.
(5) Davtyan, S. P.; Arutiunian L. A.; Shkadinskii, K. G.; Rozenberg, B. A.; Yenikolopyan, N. S. *Polym. Sci. U.S.S.R.* **1978**, *19*, 3149−3154.
(6) Davtyan, S. P.; Zhirkov, P. V.; Vol'fson, S. A. *Russ. Chem. Rev.* **1984**, *53*, 150−163.
(7) Volpert, Vit. A.; Volpert, Vl.A. *Eur. J. Appl. Math.* **1994**, *5*, 201−215.
(8) Pojman, J. A.; Craven, R.; Khan, A.; West, W. *J. Phys. Chem.* **1992**, *96*, 7466−7472.
(9) Pojman, J. A.; Willis, J.; Fortenberry, D.; Ilyashenko, V.; Khan, A. *J. Polym. Sci., Part A: Polym. Chem.* **1995**, *33*, 643−652.
(10) Pojman, J. A.; Ilyashenko, V. M.; Khan, A. M. *Physica D* **1995**, *84*, 260−268.
(11) Pojman, J. A.; Ilyashenko, V. M.; Khan, A. M. *J. Chem. Soc., Faraday Trans.* **1996**, *92*, 2825−2837.
(12) Pojman, J. A. *J. Am. Chem. Soc.* **1991**, *113*, 6284−6286.
(13) Pojman, J. A.; Khan, A. M.; West, W. *Polym. Prepr. Am Chem. Soc. Div. Polym. Chem.* **1992**, *33*, 1188−1189.
(14) Pojman, J. A.; Nagy, I. P.; Salter, C. *J. Am. Chem. Soc.* **1993**, *115*, 11044−11045.
(15) Merzhanov, A. G. Self-propagating high-temperature synthesis: twenty years of search and findings. In *Combustion and Plasma Synthesis of High-Temperature Materials*; Munir, Z. A., Holt, J. B., Eds.; VCH: New York, 1990; pp 1−53.
(16) Munir, Z. A.; Anselmi-Tamburini, U. *Mater. Sci. Rep., A Rev. J.* **1989**, *3*, 277−365.
(17) Varma, A.; J.-P. Lebrat, J.-P. *Chem. Eng. Sci.* **1992**, *47*, 2179−2194.
(18) Bazsa, G.; Epstein, I. R. *J. Phys. Chem.* **1985**, *89*, 3050−3053.
(19) Miike, H.; Muller, S. C.; Hess, B. *Phys. Rev. Lett.* **1988**, *61*, 2109−2112.
(20) Miike, H.; Muller, S. C.; Hess, B. *Chem. Phys. Lett.* **1988**, *144*, 515−520.
(21) Plesser, T.; Wilke, H.; Winters, K. H. *Chem. Phys. Lett.* **1992**, *200*, 158−162.
(22) Pojman, J. A.; Epstein, I. R. *J. Phys. Chem.* **1990**, *94*, 4966−4972.
(23) Pojman, J. A.; Epstein, I. R.; McManus, T. J.; Scowalter, K. *J. Phys. Chem.* **1991**, *95*, 1299−1306.
(24) Pojman, J. A.; Nagy, I. P.; Epstein, I. R. *J. Phys. Chem.* **1991**, *95*, 1306−1311.
(25) Vasquez, D. A.; Wilder, J. W.; Edwards, B. F. *J. Chem. Phys.* **1993**, *98*, 2138−2143.
(26) Vasquez, D. A.; Edwards, B. F.; Wilder, J. W. *Phys. Rev. A* **1991**, *43*, 6694−6699.
(27) Wilder, J. W.; Edwards, B. F.; Vasquez, D. A.; Sivashinsky, G. I. *Physica D* **1994**, *73*, 217−226.
(28) Gowariker, V. R.; Viswanathan, N. V.; Sreedhar, J. *Polymer Science*; John Wiley and Sons: New York, 1986.
(29) Manelis, G. B.; Smirnov, L. P.; Peregudov N. I. *Combust., Explosion, Shock Waves* **1977**, *13*, 389−393.
(30) Elias, H.-G. *Macromolecules*; Plenum: New York, 1977.
(31) Davtyan, S. P.; Gel'man, E. A.; Karyan, A. A.; Tonoyan, A. O.; Enikolopyan, N. S. *Dokl. Phys. Chem.* **1980**, *253*, 579−582.
(32) Gel'man, E. A.; Karyan, A. A.; Davtyan, S. P.; Vol'pert, A. I. *Dokl. Phys. Chem.* **1981**, *260*, 971−974.
(33) Aldushin, A. P.; Matkowsky, B. J.; Volpert, Vl.A. *Combust. Sci. Technol.* **1994**, *99*, 75−103.
(34) Brandrup, J., Immergut, E. H., Eds. *Polymer Handbook*; John Wiley and Sons: New York, 1982.
(35) Lyons, R. A.; Hutovic, J.; Piton, M. C.; Christie, D. I.; Clay, P. A.; Manders, B. G.; Kable, S. H.; Gilbert, R. G. *Macromolecules* **1996**, *29*, 1918−1927.